This is an Accepted Manuscript of an article published by Taylor & Francis in MECHANICS BASED DESIGN OF STRUCTURES AND MACHINES on 4/12/2019 , available online: https://doi.org/10.1080/15397734.2019.1698437

Postprint of: Kumar Jena S., Chakraverty S., Malikan M., Tornabene F.: Stability Analysis of Single-Walled Carbon Nanotubes Embedded in Winkler Foundation Placed in a Thermal Environment Considering the Surface Effect Using a New Refined Beam Theory. MECHANICS BASED DESIGN OF STRUCTURES AND MACHINES, AN INTERNATIONAL JOURNAL. (2019). DOI: 10.1080/15397734.2019.1698437

Stability Analysis of Single-Walled Carbon Nanotubes Embedded in Winkler Foundation Placed in a Thermal Environment Considering the Surface Effect Using a New Refined Beam Theory

Subrat Kumar Jena[1], S. Chakraverty[2]*, Mohammad Malikan[3], Francesco Tornabene[4]

[1, 2] Department of Mathematics, National Institute of Technology Rourkela, Odisha, 769008, India

[3]Department of Mechanics of Materials and Structures, Faculty of Civil and Environmental Engineering, Gdansk University of Technology, 80-233, ul. G. Narutowicza 11/12, Gdansk, Poland

[4] Department of Innovation Engineering, University of Salento, 73100, Lecca, Italia

*Corresponding author

E-mail:[1] sjena430@gmail.com, [2]sne_chak@yahoo.com, [3] mohammad.malikan@pg.edu.pl, [4]francesco.tornabene@unisalento.it

Abstract

This article is devoted to investigate the stability of different types of Single Walled Carbon Nanotubes (SWCNTs) such as zigzag, chiral, and armchair types which are rested in Winkler elastic foundations exposing to both the low and high temperature environments. Also, the Surface effects which include surface energy and surface residual stresses, are taken into consideration in this study. It may be noted that the surface energy aids in the increase of the flexural rigidity whereas the surface residual stresses act as distributed transverse load. Further, the proposed model is developed by considering a novel refined beam theory namely one variable first order shear

deformation beam theory along with the Hamilton's principle. Navier's method has been implemented to find out the critical buckling loads for Hinged-Hinged (H-H) boundary condition for zigzag, chiral, and armchair types of SWCNTs. A parametric study is also conducted to report the influence of various scaling parameters like small scale parameters, change in temperature, Winkler stiffness, and length to diameter ratio on critical buckling loads. Also, the present model is validated by comparing the results with other published work.

Keywords

Stability analysis; Thermal environment; Surface effect; SWCNT; Winkler foundation; Refined beam theory.

1. Introduction

A single-walled carbon nanotube (SWCNT) consists of shell body with different physical and chemical properties. SWCNTs can be considered as long graphite sheets that are wrapped in three cylindrical atomic forms which can been seen in Fig. 1(a-c) for armchair, chiral, and zigzag, respectively. Based on the rotational axis in the graphite sheet the made carbon nanotube (CNT) can be in the form of one of the cases presented in Fig. 1. These three atomic arrangements lead to different responses in nanotubes. The electronic, molecular, and structural properties of the nanotubes are derived largely from their almost one-dimensional structure. Carbon nanotubes (CNTs) are one of the strongest materials ever known to humans, both in terms of tensile resistance and elastic coefficients. This strength is derived from covalent bonds between carbon atoms. All CNTs have good thermal conductivity along their lengths, while being heat-insulating along their width and thus can transfer heat from the conductive paths. The robustness and flexibility of CNTs give them the potential to be used in the control of other nanometer structures. So they will play an important role in nanotechnology engineering. Therefore, there have been extensively studies on the prediction of their mechanical behavior.

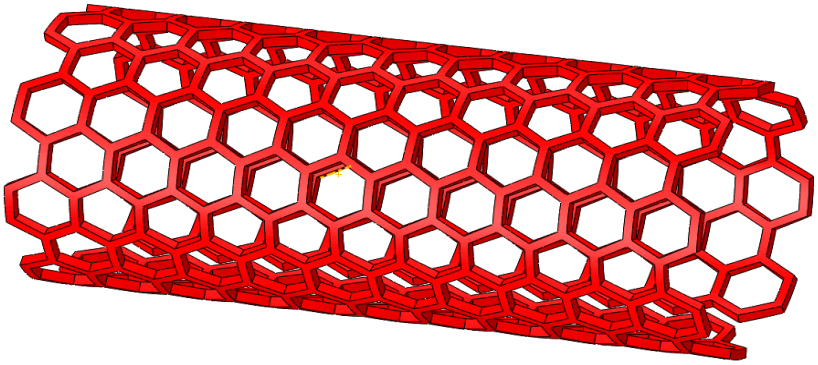

(a) Armchair

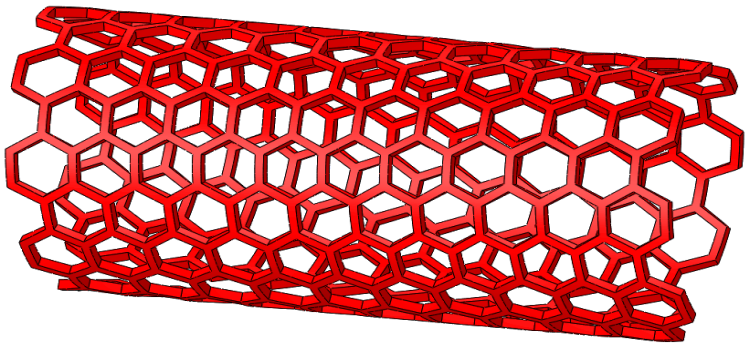

(b) Chiral

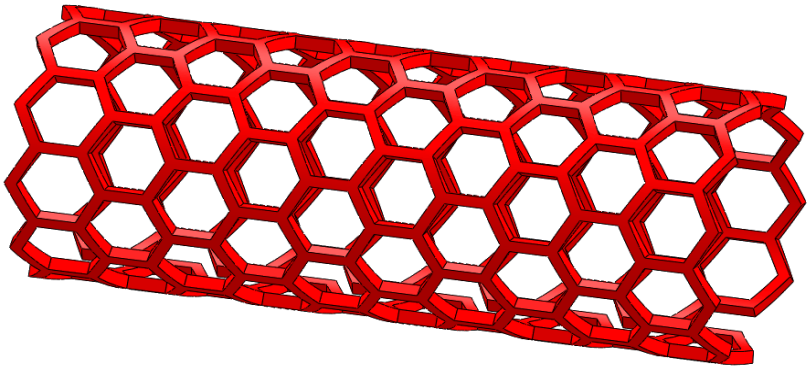

(c) Zigzag

Fig. 1. Schematically presentation of SWCNTs

Wang et al. (2006) analyzed buckling of a nano and micro tube/rod. They considered shear deformation influences based on the Timoshenko beam approach and stress nonlocality on the basis of the nonlocal elasticity. Farshi, Assadi, and Alinia-Ziazi (2010) examined effect of surface for a nanotube exposed to vibrational situations. The nanotube was assumed in the framework of

the Timoshenko beam model. They showed that the effect of surface markedly deviates the results of the natural frequency and such an effect can be significant to embed in the analysis of nanostructures. Murmu and Pradhan (2010) took effects of thermal environment on the buckling of nanotubes. The nanotube was connected on a polymer matrix and the nanoscale behavior was simulated by Eringen nonlocal theory. Lee and Chang (2010) evaluated the effects of surface on the vibrational behavior of a carbon nanotube based on the kinematic displacement field of the Timoshenko model. Pradhan and Reddy (2011) showed a stability analysis of nanotubes with only one wall while the tube was rested on a medium. The achieved mathematical relations were solved by implementing differential transformation method when different edge conditions were considered. Akgöz and Civalek (2011) proposed higher-order elasticity theory in order to analyze stability of a cantilever nanotube based on the couple stress and strain gradient models. In a brilliant study, Thai (2012) modeled carbon nanotubes as a nanobeam and investigated it mechanically in fully dynamic and static situations. The nonlocal elasticity theory, classical beam model and Hamilton principle and Navier method brought to help him to study. Wang, Hoffman, and Yu (2012) used gradient theory to consider size-dependent influences of a carbon nanotube modeled as the Timoshenko beam under mechanical stability condition. Li and Hu (2015) on the basis of the nonlocal theory of strain gradient, analytically studied small scale impacts on the stability analysis of a hinged-hinged beam in the framework of the classical beam hypothesis. The obtained numerical results were compared with the ones extracted from other size-dependent models. Zhen (2017) examined nonlocal and surface effects on the wave propagation of the nanotubes with considering the Euler-Bernoulli displacement field and internal viscosity impacts into the model. In an interesting study, She et al. (2017) calculated the critical buckling and post-buckling loads of a carbon nanotube made of functionally grading on the assuming porosity into the material. Mehralian, Tadi Beni, and Karimi Zeverdejani (2017) calibrated and validated the results of the nonlocal theory of strain gradient with the molecular mechanics in a static stability situation of carbon nanotubes whilst the nanotubes were taken into account as a nanoshell. Malikan (2019) recently presented a new beam displacement kinematic field and investigated pressurized single-walled carbon nanotubes subjected to axial loads. Bedia et al. (2019) studied the effect of strain and stress gradient on bending and buckling of nanobeam using a novel two variable shear deformation beam theory. In the work of Berghouti et al. (2019), vibration analysis of functionally graded porous nanobeam has been carried out using nth order shear deformation theory.

Medani et al. (2019) investigated static and dynamic behavior Functionally Graded Carbon Nanotubes-reinforced porous sandwich (PMPV) polymer plate using first-order shear deformation theory. Draoui et al. (2019) also used first-order shear deformation theory to study both static and dynamic characteristics of carbon nanotube-reinforced composite sandwich plates. Semmah et al. (2019) analytically investigated thermal stability of zigzag single-walled boron nitride nanotube embedded in an elastic medium using first-order shear deformation theory. Draiche et al. (2019) used simple first order shear deformation theory to study static behavior of laminated reinforced composite plates analytically using both the sinusoidal and uniform loads. Chaabane et al. (2019), with the help of hyperbolic shear deformation theory analyzed static and dynamic characteristics of functionally graded beam embedded in an elastic foundation. The studies on the mechanical analysis of carbon nanotubes are not limited to the mentioned ones and there can be found other important works (Chang and Lee 2013, Larbi et al. 2013, Teifouet, Robinson, and Adali 2017, Chen, Fang, and Wang 2017, Malikan 2017, Arefi and Arani 2018, Malikan and Nguyen 2018, Malikan, Nguyen, and Tornabene 2018a, Malikan, Nguyen, and Tornabene. 2018b, Malikan and Dastjerdi 2018, Malikan, Tornabene, and Dimitri 2018, Jena and Chakraverty 2018a, Jena and Chakraverty 2018b, Jena and Chakraverty 2018c, Dastjerdi, and Tadi Beni 2019, Malikan, Dimitri, and Tornabene 2019, Fattahi, Sahmani, and Ahmed. 2019, Malikan et al. 2019, Sun and Li 2019, Jena and Chakraverty 2019a, Jena and Chakraverty 2019b, Jena and Chakraverty 2019c, Jena et al. 2019, Jena, Chakraverty, and Tornabene 2019a, Jena, Chakraverty, and Tornabene 2019b, Jena, Chakraverty, and Tornabene 2019c, Jena, Chakraverty, and Jena. 2019, Jena, Chakraverty, and Malikan 2019).

In this research, three different frameworks for SWCNTs have been considered, such as chiral, armchair, and zigzag carbon nanotubes, which are exposed to thermal environment. In addition to this, surface effects of the nanostructures are here taken into investigation. On the other hand, the nanotube is embedded in a polymer substrate, namely Winkler foundation. To predict the motion of the model's nodes, the field of displacements along two axes is utilized as a new refined beam model. After formulating, there have been obtained the required thermal stability equations in order to consider analytically the Hinged-Hinged (H-H) nanotube with presenting outcomes numerically. Also, a parametric study has been carried out to witness the impact of various parameters such as small scale parameters, change in temperature, Winkler stiffness, and length to diameter ratio on critical buckling loads.

2. Proposed model

In this model, a SWCNT having length L, outer diameter d_o, inner diameter d_i, and wall thickness t are considered. The mechanical properties of the SWCNT are E, ρ, and υ which denote the Young's modulus, mass density, and Poisson's ratio, respectively. E_i, and t_i denote the Young's modulus and thickness of the inner surface layer whereas E_o, and t_o designate the Young's modulus and thickness of the outer surface layer and the schematic diagrams can be seen in Figs. (2-3). Fig. 2. illustrates the schematic presentation of continuum nanotube model whereas Fig.3. depicts the atomic model of armchair CNT.

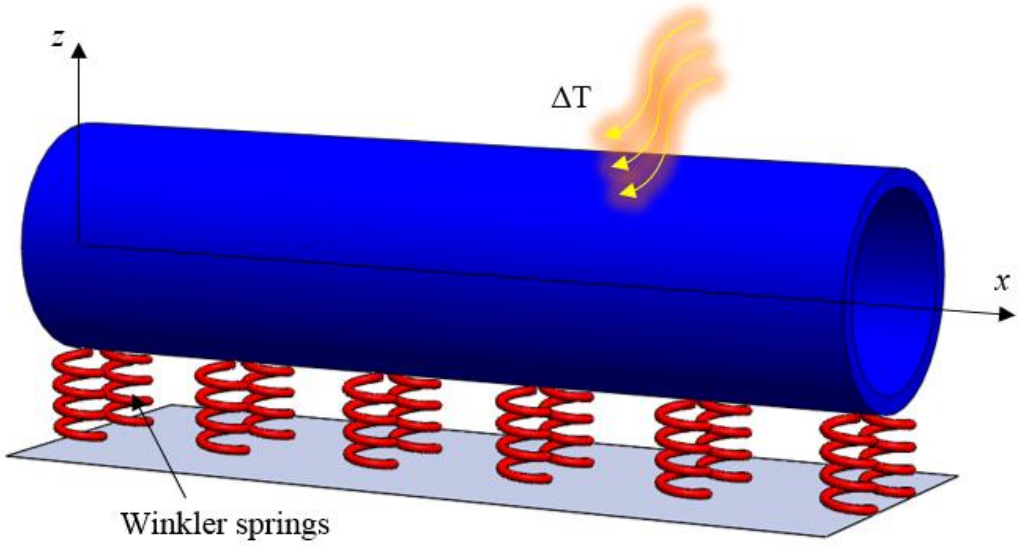

Fig. 2. Schematic presentation of continuum nanotube placed on the Winkler foundation

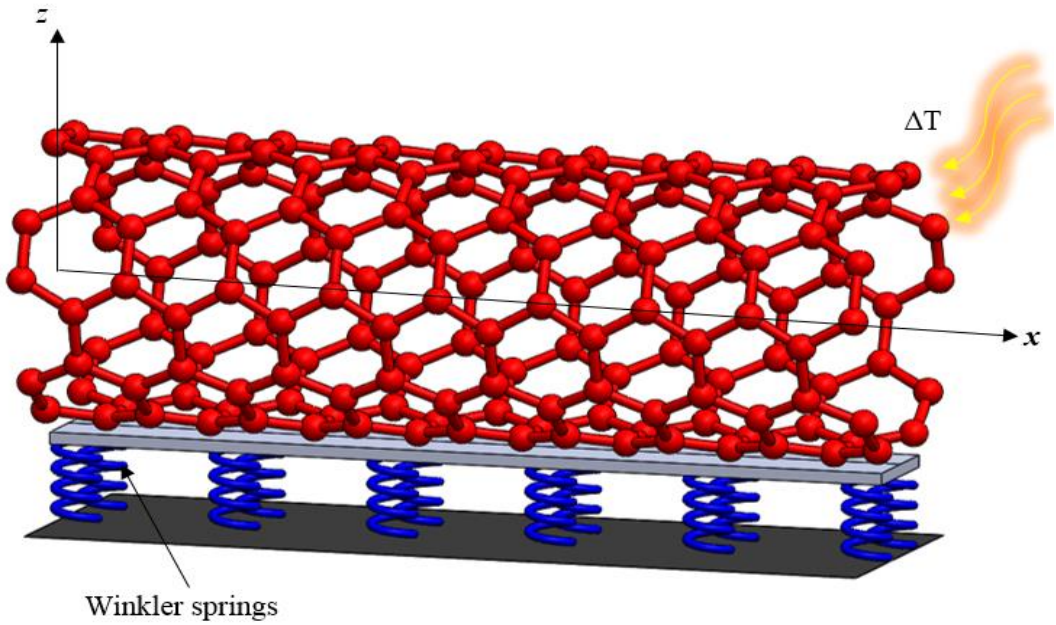

Fig. 3. Schematic presentation of atomic model of armchair CNT placed on the Winkler foundation

In order to study the effects of the both the layers we have assumed that $E_i t_i = E_o t_o$, which is equal to $E_s t_0$ as a material property of the SWCNT. Surface effects which include surface energy and surface residual stresses, influence the dynamical behaviors of nanostructures considerably. Moreover, the surface energy aids in the increase of the flexural rigidity whereas the surface residual stresses act as distributed transverse load. The flexural rigidity or bending rigidity due to surface energy may be stated as (Farshi, Assadi, and Alinia-Ziazi 2010, Zhen 2017)

$$(EI)^{se} = \frac{\pi}{8} E_s t_0 \left(d_o^3 + d_i^3\right), \tag{1}$$

Now, the effective flexural rigidity of the nanotube is obtained as (Farshi, Assadi, and Alinia-Ziazi 2010, Zhen 2017)

$$(EI)^{eff} = (EI) + (EI)^{se} = (EI) + \frac{\pi}{8} E_s t_0 \left(d_o^3 + d_i^3\right) \tag{2}$$

The distributed transverse load due to surface residual stresses as per Laplace-Young equation, is presented as (Farshi, Assadi, and Alinia-Ziazi 2010, Zhen 2017)

$$q(x) = 2\tau\left(d_o + d_i\right)\frac{\partial^2 w}{\partial x^2} \tag{3}$$

Here τ is surface tension due to residual stresses.

The displacement fields, as per new refined beam theory can be expressed as (Malikan and Dastjerdi 2018, Malikan, Nguyen, and Tornabene 2018a, Malikan, Dimitri, and Tornabene 2019)

$$\begin{aligned} u_1(x,z,t) &= u(x,t) - z\frac{\partial w(x,t)}{\partial x} \\ u_2(x,z,t) &= 0 \\ u_3(x,z,t) &= w(x,t) + B\frac{\partial^2 w(x,t)}{\partial x^2} \end{aligned} \tag{4}$$

In which $u(x,t)$ and $w(x,t)$ are the displacements of the neutral axis in axial and transverse directions, respectively. $B = \frac{EI}{AG}$, where E is the Young's modulus, $I = \int_A z^2\, dA$ is the moment of area, A is the area of cross-section, and G is the shear modulus. Considering Von Kármán hypothesis, the strain displacement relations are given as

$$\begin{aligned} \varepsilon_{xx} &= \frac{\partial u}{\partial x} - z\frac{\partial^2 w}{\partial x^2} + \frac{1}{2}\left(B\frac{\partial^3 w}{\partial x^3} + \frac{\partial w}{\partial x}\right)^2 - \alpha_x \Delta T \\ \gamma_{xz} &= B\frac{\partial^3 w}{\partial x^3} \end{aligned} \tag{5}$$

Here $\alpha_x \Delta T$ is the thermal axial strain along x-axis and α_x is the coefficient of thermal expansion.

The virtual strain energy (δU) may be written as

$$\delta U = \iiint_V \left(\sigma_{xx}\delta\varepsilon_{xx} + \sigma_{xz}\delta\gamma_{xz}\right)dV$$

$$= \int_0^L \left[\begin{array}{l} N_{xx}\dfrac{\partial\delta u}{\partial x} - M_{xx}\dfrac{\partial^2\delta w}{\partial x^2} + Q_{xz}B\dfrac{\partial^3\delta w}{\partial x^3} + \\ N_{xx}\left(B^2\dfrac{\partial^3 w}{\partial x^3}\dfrac{\partial^3\delta w}{\partial x^3} + B\dfrac{\partial^3 w}{\partial x^3}\dfrac{\partial\delta w}{\partial x} + B\dfrac{\partial w}{\partial x}\dfrac{\partial^3\delta w}{\partial x^3} + \dfrac{\partial w}{\partial x}\dfrac{\partial\delta w}{\partial x}\right) \end{array}\right]dx \tag{6}$$

$$= \int_0^L \left[\begin{array}{l} -\dfrac{\partial N_{xx}}{\partial x}\delta u + \dfrac{\partial^2 M_{xx}}{\partial x^2}\delta w - B\dfrac{\partial^3 Q_{xz}}{\partial x^3}\delta w - B^2\left(\dfrac{\partial^3}{\partial x^3}\left(N_{xx}\dfrac{\partial^3 w}{\partial x^3}\right)\right)\delta w \\ -B\left(\dfrac{\partial}{\partial x}\left(N_{xx}\dfrac{\partial^3 w}{\partial x^3}\right)\right)\delta w - B\left(\dfrac{\partial^3}{\partial x^3}\left(N_{xx}\dfrac{\partial w}{\partial x}\right)\right)\delta w - \dfrac{\partial}{\partial x}\left(N_{xx}\dfrac{\partial w}{\partial x}\right)\delta w \end{array}\right]dx$$

where $M_{xx} = \int_A z\sigma_{xx}dA$, $N_{xx} = \int_A \sigma_{xx}dA$, and $Q_{xz} = \int_A \sigma_{xz}dA$ are the local stress resultants of the beam.

The virtual work done (δW) by external loads is defined as

$$\delta W = \int_0^L \left[2\tau\left(d_o + d_i\right)\left(\frac{\partial^2 w}{\partial x^2}\right) - k_w w - \left(\frac{EA\alpha_x}{1-2\nu}\Delta T\right)\left(\frac{\partial^2 w}{\partial x^2}\right)\right]\delta w dx, \tag{7}$$

where k_w is the Winkler modulus, α_x is the coefficient of thermal expansion, ΔT is the change in temperature, and ν is the Poisson's ratio of the nanotube.

Substituting Eqs. (6-7) in the Hamilton's principle $\delta\prod = \int_0^t \delta\left(U + W\right)dt$, and assigning $\delta\prod$ to zero, we obtain the equations of motion as

$$\left[\begin{array}{l} -\dfrac{\partial^2 M_{xx}}{\partial x^2} + B\dfrac{\partial^3 Q_{xz}}{\partial x^3} + N_{xx}\left(B^2\dfrac{\partial^6 w}{\partial x^6} + 2B\dfrac{\partial^4 w}{\partial x^4} + \dfrac{\partial^2 w}{\partial x^2}\right) - \\ 2\tau\left(d_o + d_i\right)\left(\dfrac{\partial^2 w}{\partial x^2}\right) + k_w w + \left(\dfrac{EA\alpha_x}{1-2\nu}\Delta T\right)\left(\dfrac{\partial^2 w}{\partial x^2}\right) \end{array}\right] = 0 \tag{8}$$

The local stress resultants, using Hookean stress-strain elasticity relation can be rewritten as

$$M_{xx} = -EI\frac{\partial^2 w}{\partial x^2}$$
$$Q_{xz} = AGB\frac{\partial^3 w}{\partial x^3} \tag{9}$$

From the Eringen's nonlocal elasticity theory (Eringen 1972), we have

$$\left(1-(e_0 a)^2\frac{\partial^2}{\partial x^2}\right)\sigma_{ij} = C_{ijkl}\varepsilon_{kl} \tag{10}$$

In which $\sigma_{ij}, \varepsilon_{kl}$ and C_{ijkl} are stress tensor, strain tensor and elastic modulus constant, respectively.

Combining Eq. (9) with Eq. (10), the nonlocal stress resultants may be given as

$$\left(1-(e_0 a)^2\frac{\partial^2}{\partial x^2}\right)M_{xx} = -EI\frac{\partial^2 w}{\partial x^2} \tag{11.a}$$

$$\left(1-(e_0 a)^2\frac{\partial^2}{\partial x^2}\right)Q_{xz} = AGB\frac{\partial^3 w}{\partial x^3} \tag{11.b}$$

Implementing Eq. (11) in Eq. (8), the governing equation of motion is expressed as

$$\left(1-(e_0 a)^2\frac{\partial^2}{\partial x^2}\right)\left[\begin{array}{l} -N_{xx}\left(B^2\frac{\partial^6 w}{\partial x^6}+2B\frac{\partial^4 w}{\partial x^4}+\frac{\partial^2 w}{\partial x^2}\right)-k_w w+ \\ 2\tau(d_o+d_i)\left(\frac{\partial^2 w}{\partial x^2}\right)-\left(\frac{EA\alpha_x}{1-2\nu}\Delta T\right)\left(\frac{\partial^2 w}{\partial x^2}\right)+ \end{array}\right] = EI\frac{\partial^4 w}{\partial x^4}+AGB^2\frac{\partial^6 w}{\partial x^6} \tag{12}$$

Considering the surface energy, i.e. Eq. (2) in the governing Eq. (12), we obtain

$$\left(1-(e_0 a)^2\frac{\partial^2}{\partial x^2}\right)\left[\begin{array}{l} -N_{xx}\left(B^{*2}\frac{\partial^6 w}{\partial x^6}+2B^*\frac{\partial^4 w}{\partial x^4}+\frac{\partial^2 w}{\partial x^2}\right)-k_w w \\ +2\tau(d_o+d_i)\left(\frac{\partial^2 w}{\partial x^2}\right)-\left(\frac{EA\alpha_x}{1-2\nu}\Delta T\right)\left(\frac{\partial^2 w}{\partial x^2}\right) \end{array}\right] = (EI)^{eff}\frac{\partial^4 w}{\partial x^4}+AGB^{*2}\frac{\partial^6 w}{\partial x^6} \tag{13}$$

In which $B^* = \frac{(EI)^{eff}}{AG}$ and $(EI)^{eff} = (EI)+(EI)^{se}$, where $(EI)^{se}$ is the flexural rigidity due to surface energy.

In order to study the stability of SWCNT , the in-plane force resultant $(N_{xx})$is replaced by $-P$ in Eq. (13) and the governing equation is given as

$$\left(1-(e_0a)^2\frac{\partial^2}{\partial x^2}\right)\begin{bmatrix} P\left(B^{*2}\frac{\partial^6 w}{\partial x^6}+2B^*\frac{\partial^4 w}{\partial x^4}+\frac{\partial^2 w}{\partial x^2}\right) \\ +2\tau(d_o+d_i)\left(\frac{\partial^2 w}{\partial x^2}\right)-k_w w \\ -\left(\frac{EA\alpha_x}{1-2\nu}\Delta T\right)\left(\frac{\partial^2 w}{\partial x^2}\right)\end{bmatrix}=(EI)^{eff}\frac{\partial^4 w}{\partial x^4}+AGB^{*2}\frac{\partial^6 w}{\partial x^6} \tag{14}$$

3. Analytical Method

The Navier's method has been used to solve the governing equation analytically for Simply Supported boundary condition. According to Navier's approach the transverse displacement (w) , may be expressed as (Malikan and Dastjerdi 2018, Malikan, Nguyen, and Tornabene 2018a, Malikan, Dimitri, and Tornabene 2019)

$$w(x,t)=\sum_{n=1}^{\infty}W_n\sin\left(\frac{n\pi}{L}x\right)e^{i\omega_n t} \tag{15}$$

In which W_n, and ω_n are the displacement and frequency of the beam.

Substituting Eq. (15) in Eq. (14), the buckling load can be obtained as

$$P_n=\frac{\begin{array}{l}2\tau(d_o+d_i)\left(\frac{n\pi}{L}\right)^2+2\tau(d_o+d_i)(e_0a)^2\left(\frac{n\pi}{L}\right)^4+k_w+(e_0a)^2k_w\left(\frac{n\pi}{L}\right)^2 \\ -\left(\frac{EA\alpha_x}{1-2\nu}\Delta T\right)\left(\frac{n\pi}{L}\right)^2-\left(\frac{EA\alpha_x}{1-2\nu}\Delta T\right)(e_0a)^2\left(\frac{n\pi}{L}\right)^4+(EI)^{eff}\left(\frac{n\pi}{L}\right)^4-AGB^{*2}\left(\frac{n\pi}{L}\right)^6\end{array}}{\begin{array}{l}\left\langle -B^{*2}\left(\frac{n\pi}{L}\right)^6+2B^*\left(\frac{n\pi}{L}\right)^4-\left(\frac{n\pi}{L}\right)^2\right\rangle+(e_0a)^2 \\ \left\langle -B^{*2}\left(\frac{n\pi}{L}\right)^8+2B^*\left(\frac{n\pi}{L}\right)^6-\left(\frac{n\pi}{L}\right)^4\right\rangle\end{array}} \tag{16}$$

4. Results and discussion

Three different types of SWCNTs have been considered in this study which includes zigzag, chiral and armchair nanotubes. The diameters of the nanotubes with chirality indices $(n,\ m)$ are given by

Zhen (2017) as $d = \frac{a}{\pi}\sqrt{3\left(n^2 + m^2 + mn\right)}$, where '$a$' is the internal characteristics length or C-C bond length which is equal to $0.142nm$. In this regards, we have considered zigzag nanotube (Zhen 2017) with chirality indices $(21, 0)$ and the corresponding diameter is $d = 1.64nm$, chiral nanotube (Zhen 2017) is having chirality indices $(18, 9)$ with diameter $d = 1.86nm$ whereas the chirality indices of the armchair nanotube (Zhen 2017) is assumed as $(16, 16)$ with diameter $d = 2.17nm$. The natural frequencies (ω) and critical buckling loads (P_{cr}) of for the above mentioned SWCNTs have calculated by implementing Navier's methods for Hinged-Hinged (H-H) boundary condition. Further, the Young's modulus $E = 1TPa$, the wall thickness of the nanotube $t = 0.34nm$, the mass density $\rho = 1370Kg/m^3$, surface tension due to residual stresses $\tau = 0.31N/m$, Poisson's ratio $\nu = 0.19$ and $E_s t_0 = 35.3N/m$ have been considered from Zhen (2017) for the parametric study.

4.1 Validation

To validate the proposed model, the critical buckling loads (P_{cr}) obtained from Eq. (16), has been now compared with the results reported in Malikan and Dastjerdi (2018) in special cases which is presented Table 1. These tabular results are computed using Navier's method for Hinged-Hinged (H-H) boundary condition by taking Young's modulus $E = 1TPa$, Poisson's ratio $(\nu) = 0.18$, and diameter $(d) = 1nm$ with no effect of surface energy, surface residual stresses, and thermal environment. Table 1 reveals that the present results obtained by the proposed model is showing very good agreement with Malikan and Dastjerdi (2018).

Table 1 Validation of critical buckling load (P_{cr}) with Malikan and Dastjerdi (2018)

$e_0 a$	(P_{cr})(Present)				(P_{cr})(Malikan and Dastjerdi 2018)			
	$L = 14$	$L = 16$	$L = 18$	$L = 20$	$L = 14$	$L = 16$	$L = 18$	$L = 20$
0	2.4905	1.9034	1.5021	1.2156	2.4905	1.9034	1.5021	1.2156
0.5	2.4595	1.8852	1.4907	1.2082	2.4595	1.8852	1.4907	1.2082
1	2.3711	1.8327	1.4577	1.1864	2.3711	1.8327	1.4577	1.1864

1.5	2.2370	1.7515	1.4057	1.1517	2.2370	1.7515	1.4057	1.1517
2	2.0729	1.6494	1.3389	1.1064	2.0729	1.6494	1.3389	1.1064

4.2 Effect of small scale parameter

This subsection is devoted to study the effects of small scale parameters $(e_0 a)$ on the critical buckling loads (P_{cr}) for three different types of SWCNTs which include zigzag, chiral and armchair. This study is conducted in both the low or room temperature environment with the coefficient of thermal expansion $\alpha_x = -1.6\times10^{-6}\,K^{-1}$ (Murmu and Pradhan 2010) as well as high temperature environment with $\alpha_x = 1.1\times10^{-6}\,K^{-1}$ (Murmu and Pradhan 2010). In this regards, both the tabular and graphical results are presented in Table 2 and Figs. 4-5. These results are calculated by assuming the Winkler modulus $k_w = 1GPa$, length to diameter ratio $\frac{L}{d} = 5$, and change in temperature $\Delta T = 50K$ for both the low and temperature environments. Here, the small scale parameters have been varied from 0 to 2 nm with an increment of 0.5. Table 2 represents the variation of critical buckling loads with small scale parameters whereas Figs. 4-5 represent the variation of $\chi_{e_0 a}$ which is defined as the ratio of critical buckling load with nonlocal effects and critical buckling load without nonlocal effects with $e_0 a$. From these studies, it is observed that critical buckling load decreases with the increment of nonlocal effects in both the room and high temperature environments. Also, armchair type of carbon nanotubes possesses highest critical buckling loads while zigzag possesses the lowest value.

Table 2 Critical buckling load (P_{cr}) in nN with $k_w = 1GPa$, $\frac{L}{d} = 5$, with $\Delta T = 50K$

$e_0 a$	Low temperature Environment $(\alpha_x = -1.6\times10^{-6}K^{-1})$			High temperature Environment $(\alpha_x = 1.1\times10^{-6}K^{-1})$		
	Zigzag	Chiral	Armchair	Zigzag	Chiral	Armchair
0	73.3473	90.0240	114.8223	73.1617	89.8053	114.5563
0.5	71.1209	87.8961	112.8326	70.9354	87.6774	112.5666

1	65.2967	82.1663	107.3253	65.1111	81.9476	107.0593
1.5	57.7318	74.3509	99.4413	57.5462	74.1321	99.1753
2	50.0793	65.9811	90.4826	49.8938	65.7623	90.2166

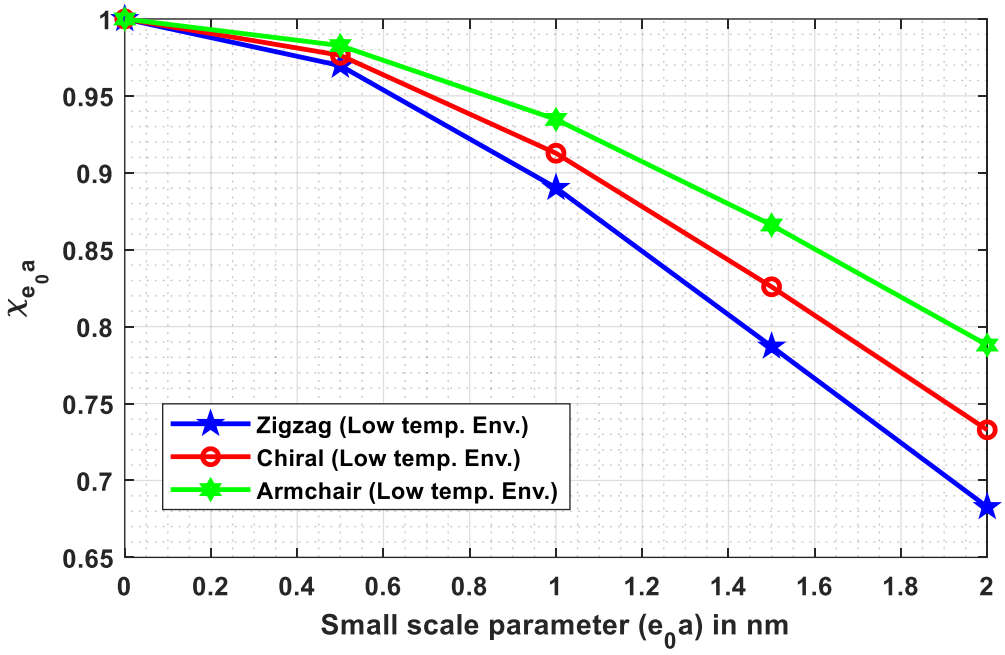

Fig. 4. $\chi_{e_0 a}$ Vs. $e_0 a$ in low temperature environment

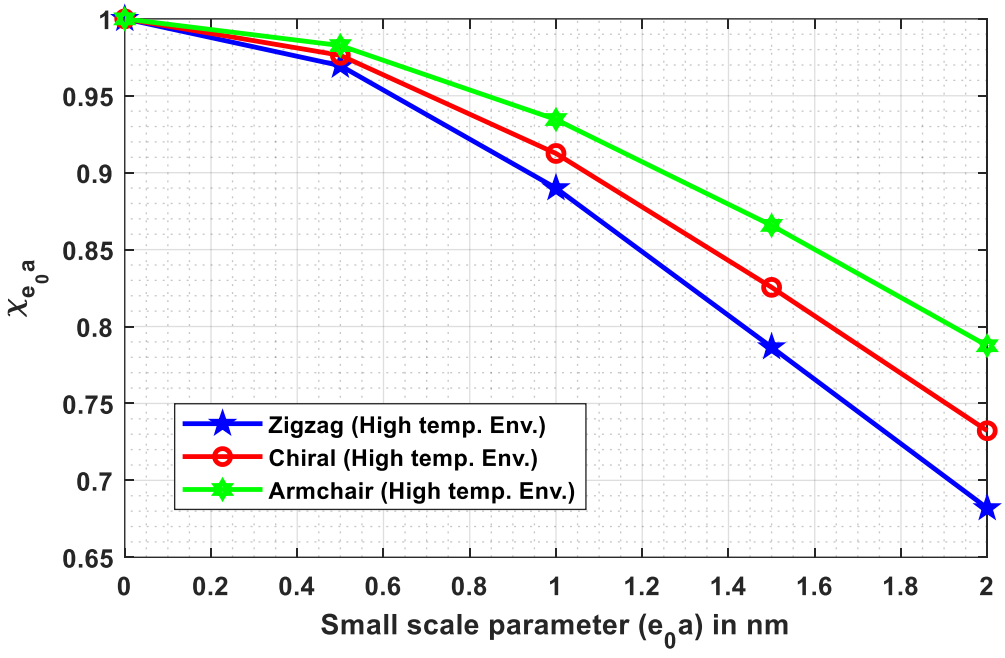

Fig. 5. $\chi_{e_0 a}$ Vs. $e_0 a$ in high temperature environment

4.3 Effect of thermal environments

The impacts of thermal environments and change in temperatures ΔT on critical buckling loads (P_{cr}) have studied through this subsection for zigzag, chiral, and armchair CNTs considering H-H boundary condition which is depicted in Table 3 and Figs. 6-7. In this regard, we have considered the Winkler modulus $k_w = 1GPa$, length to diameter ratio $\frac{L}{d} = 5$, and nonlocal parameter $e_0 a = 1nm$. The change in temperatures ΔT are taken as 0 K, 50 K, 100 K, 150 K, and 200 K. Table 3 represent the variation of critical buckling loads with change in temperature ΔT whereas Figs. 6-7 illustrate the effect of ΔT on $\chi_{\Delta T}$, which is defined as the ratio of critical buckling load with change in temperature ΔT and critical buckling load without considering the effect ΔT in both the room temperature and high temperature environments. From these results, it can be concluded that critical buckling loads increase with the rise of change in temperature ΔT in low temperature environments whereas this scenario is completely different in case of high temperature environment, i.e. critical buckling loads decrease with the increase of ΔT. Also, this trend remains same for zigzag, chiral, and armchair CNTs.

Table 3 Critical buckling load (P_{cr}) in nN with $k_w = 1GPa$, $\frac{L}{d} = 5$, and $e_0 a = 1nm$

ΔT	Low temperature Environment $(\alpha_x = -1.6\times10^{-6}K^{-1})$			High temperature Environment $(\alpha_x = 1.1\times10^{-6}K^{-1})$		
	Zigzag	Chiral	Armchair	Zigzag	Chiral	Armchair
0	65.1867	82.0367	107.1677	65.1867	82.0367	107.1677
50	65.2967	82.1663	107.3253	65.1111	81.9476	107.0593
100	65.4066	82.2960	107.4829	65.0355	81.8585	106.9509
150	65.5165	82.4256	107.6406	64.9600	81.7693	106.8426
200	65.6265	82.5552	107.7982	64.8844	81.6802	106.7342

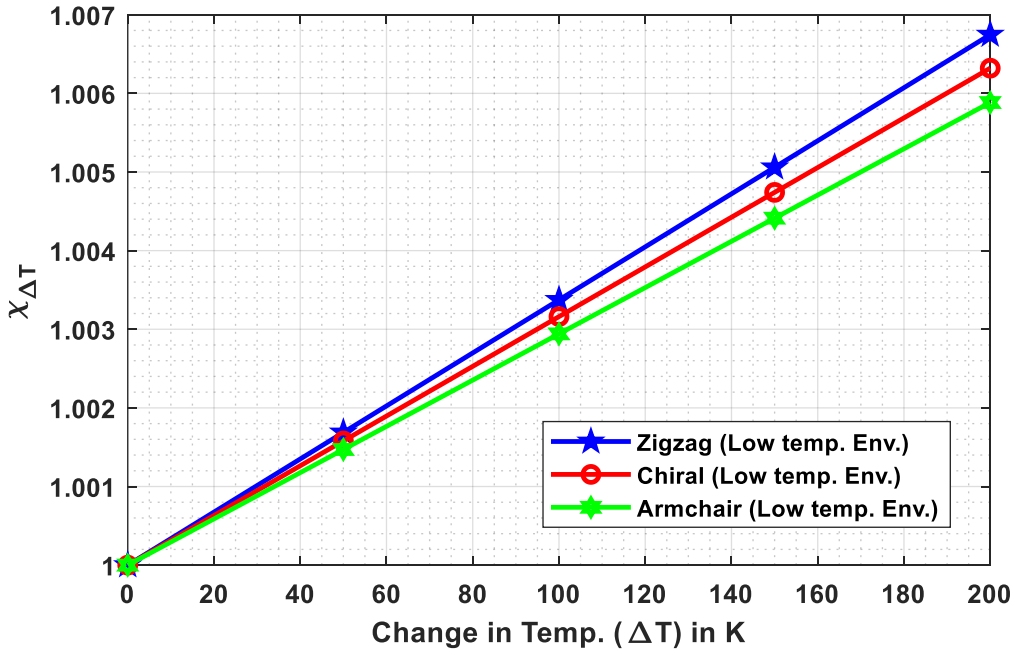

Fig. 6. $\chi_{\Delta T}$ Vs. ΔT in low temperature environment

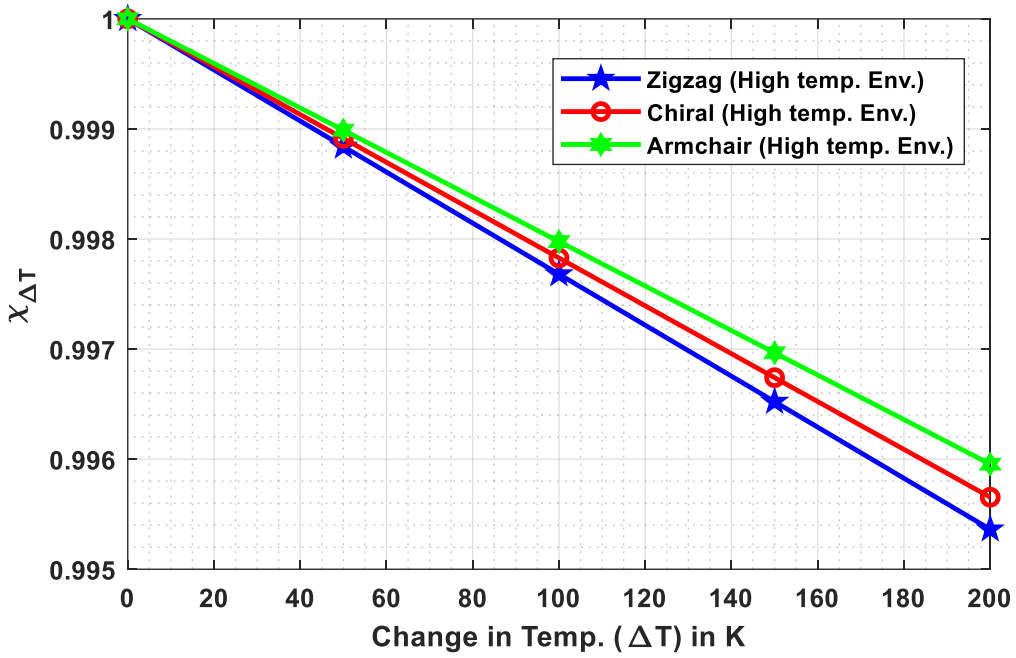

Fig. 7. $\chi_{\Delta T}$ Vs. ΔT in high temperature environment

4.4 Effect of Winkler modulus

Influences of Winkler modulus (w_k) is reported through this subsection by conducting a parametric study for three different types of SWCNTs considering both the surface energy and surface residual stresses. Further, the study is conducted in both the room temperature and high temperature with $\Delta T = 50K$, $\frac{L}{d} = 5$, $e_0 a = 1nm$ and the Winkler modulus (w_k) is taken as 0 GPa, 1 GPa, 2 GPa, 3 GPa, 4 GPa. Table 4 and Figs. 8-9 are the tabular and graphical representations of the study where Fig. 5 is the graphical results for room temperature while Fig. 6 is for high temperature environment. The Critical buckling loads (P_{cr}), for all the types of chirality indices and in low and high temperature, increase with increasing the stiffness of elastic foundation which can be clearly witnessed from the Table 4 and Figs. 8-9.

Table 4 Critical buckling load (P_{cr}) in nN with $\Delta T = 50K$, $\frac{L}{d} = 5$, and $e_0 a = 1nm$

k_w	Low temperature Environment $\left(\alpha_x = -1.6\times10^{-6}K^{-1}\right)$			High temperature Environment $\left(\alpha_x = 1.1\times10^{-6}K^{-1}\right)$		
	Zigzag	Chiral	Armchair	Zigzag	Chiral	Armchair
0	56.9357	71.3212	92.4163	56.7502	71.1025	92.1503
1	65.2967	82.1663	107.3253	65.1111	81.9476	107.0593
2	73.6576	93.0114	122.2343	73.4721	92.7927	121.9683
3	82.0185	103.8566	137.1433	81.8330	103.6378	136.8773
4	90.3795	114.7017	152.0523	90.1940	114.4829	151.7863

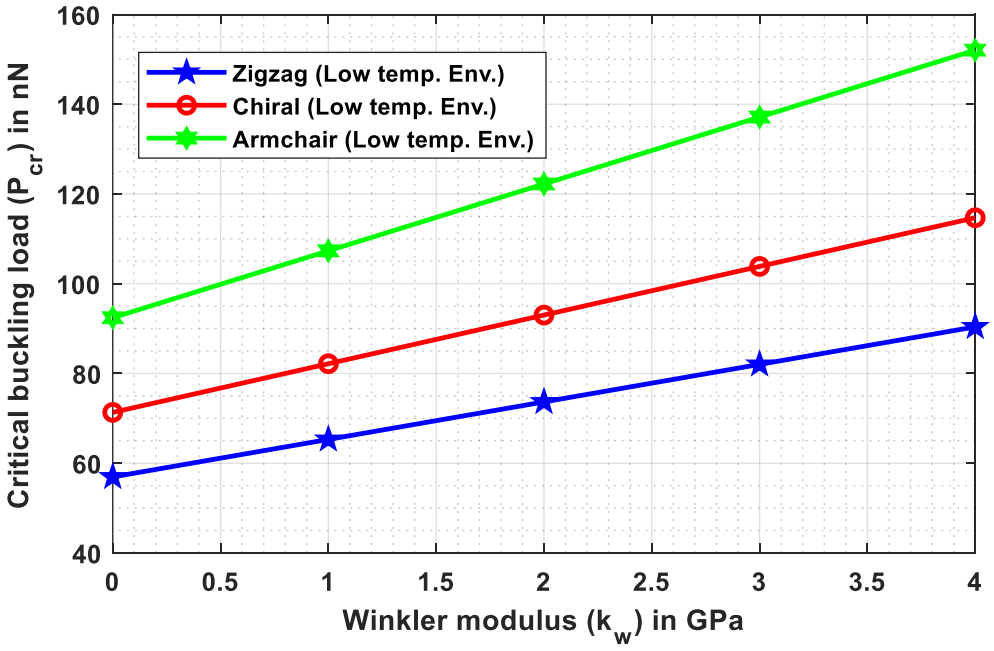

Fig. 8. P_{cr} Vs. k_w in low temperature environment

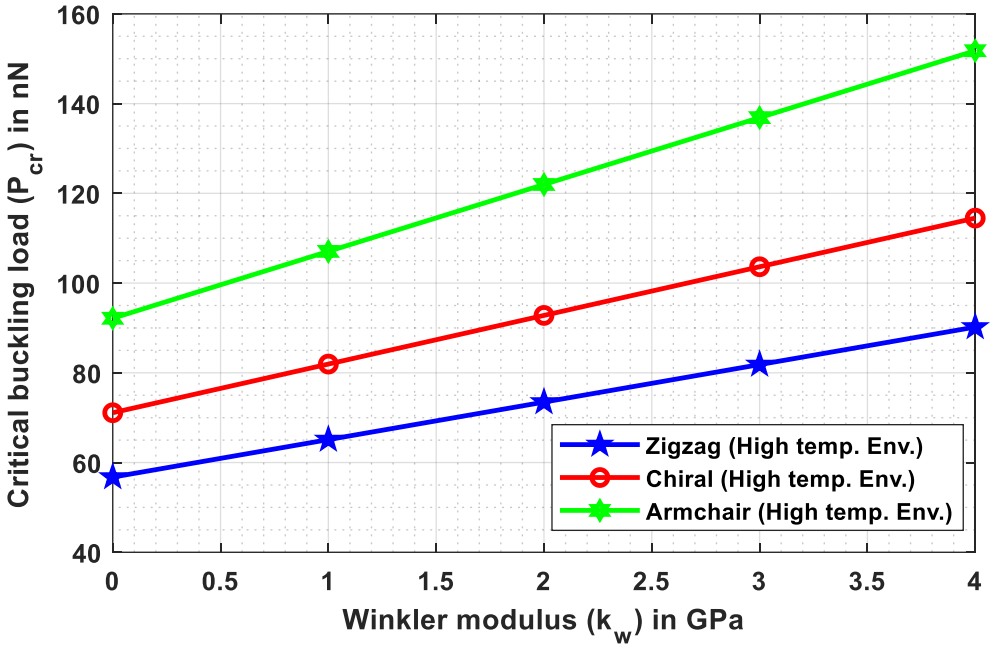

Fig. 9. P_{cr} Vs. k_w in high temperature environment

4.5 Effect of length to diameter ratio

Length to diameter ratio $\left(\frac{L}{d}\right)$ also influences the critical buckling load significantly. Thus, this subsection is devoted to investigate the impacts length to height ratio on critical buckling load. For computation purpose, we have considered $\Delta T = 50K$, $k_w = 1GPa$, $e_0 a = 1nm$ while $\left(\frac{L}{d}\right)$ is taken as 5, 7.5, 10, 12.5, 15. Table 5 represent the tabular results of the variations of (P_{cr}) with $\frac{L}{d}$ whereas Fig. 10 and Fig. 11 demonstrate the graphical results of variations for low and high temperature respectively. From this results, it is very interesting to note that the critical buckling loads show some unusual behavior in response to the length to diameter ratio, i.e. at first, the (P_{cr}) decreases and then it increases steadily. This response remains same for all the SWCNTs which includes zigzag, chiral and armchair type with both the environment which can be perceived clearly from the study.

Table 5 Critical buckling load (P_{cr}) in nN with $\Delta T = 50K$, $k_w = 1GPa$, $e_0 a = 1nm$

$\frac{L}{d}$	Low temperature Environment $\left(\alpha_x = -1.6\times10^{-6}K^{-1}\right)$			High temperature Environment $\left(\alpha_x = 1.1\times10^{-6}K^{-1}\right)$		
	Zigzag	Chiral	Armchair	Zigzag	Chiral	Armchair
5	65.2967	82.1663	107.3253	65.1111	81.9476	107.0593
7.5	43.3648	54.3396	71.1542	43.1997	54.1458	70.9199
10	44.4481	56.1852	74.6621	44.2893	55.9991	74.4376
12.5	54.7100	69.6558	93.5320	54.5540	69.4731	93.3118
15	70.6775	90.3589	122.0220	70.5230	90.1781	121.8041

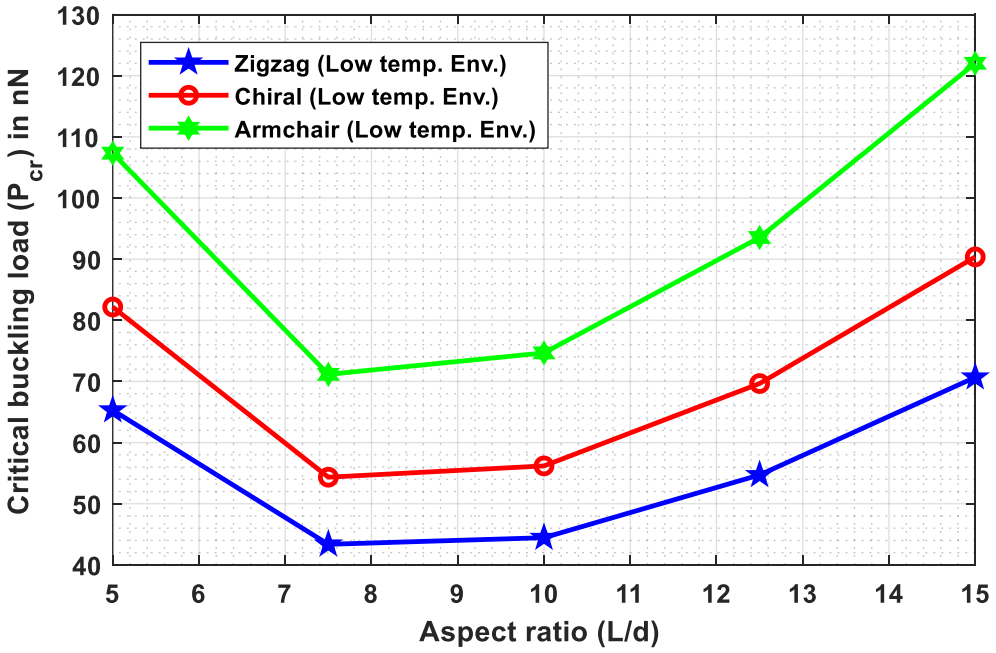

Fig. 10. P_{cr} Vs. $\frac{L}{d}$ in low temperature environment

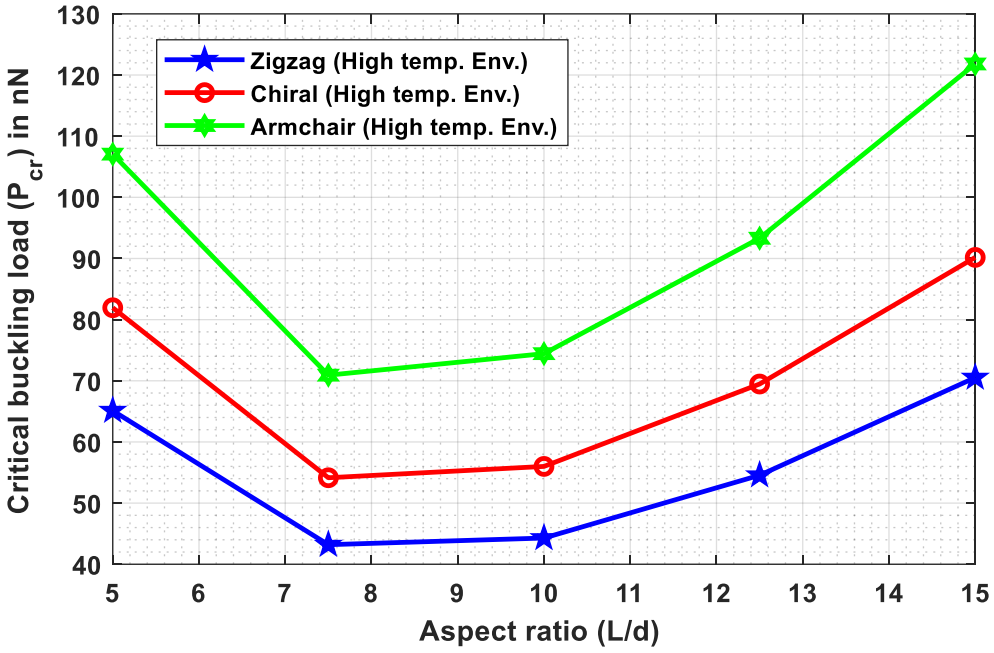

Fig. 11. P_{cr} Vs. $\frac{L}{d}$ in high temperature environment

5 Concluding remarks

In this article, stability analysis of zigzag, chiral, and armchair types of CNTs are conducted, considering the surface effects and thermal environments, which are embedded in Winkler elastic foundations. A new refined beam theory along with Hamilton's principle have been utilized to develop the proposed model for investigations. The critical buckling loads are calculated analytically from the governing equation using Navier's approach for H-H boundary condition. Followings are the main comments;

- The armchair carbon nanotubes possess the highest critical buckling loads while the zigzag carbon nanotubes are having the lowest critical buckling loads.
- The critical buckling loads decrease with the increment of nonlocal parameters for all types of CNT in both the room and high temperature environments.
- The critical buckling loads increase with the rise of change in temperature in low temperature environments whereas it is completely opposite in case of high temperature environment.
- The Critical buckling loads increase with increasing the stiffness of elastic foundation for all the types of CNTs.

- The critical buckling loads show some unusual behavior with respect to the length to diameter ratio, initially, it decreases and then it increases steadily. This response remains same for all the SWCNTs in any environments.

Acknowledgment

The first two authors are very much thankful to Defence Research & Development Organization (DRDO), New Delhi, India (Sanction Code: DG/TM/ERIPR/GIA/17-18/0129/020) for the funding to carry out the present research work.

References

Akgöz, B., and Ö. Civalek. 2011. Buckling analysis of cantilever carbon nanotubes using the strain gradient elasticity and modified couple stress theories. *Journal of Computational and Theoretical Nanoscience* 8:1821-1827.

Arefi, Mohammad, and Amir Hossein Soltan Arani. 2018 Higher order shear deformation bending results of a magnetoelectrothermoelastic functionally graded nanobeam in thermal, mechanical, electrical, and magnetic environments. *Mechanics Based Design of Structures and Machines* 46(6):669-692.

Berghouti, H., E. A. Adda Bedia, A. Benkhedda, and A. Tounsi. 2019. Vibration analysis of nonlocal porous nanobeams made of functionally graded material. *Advances in nano research* 7(5):351-64.

Bedia, W. A., M. S. Houari, A. Bessaim, A. A. Bousahla, A. Tounsi, T. Saeed, and M. S. Alhodaly. 2019. A New Hyperbolic Two-Unknown Beam Model for Bending and Buckling Analysis of a Nonlocal Strain Gradient Nanobeams. *Journal of Nano Research* 57:175-191.

Chaabane, L. A., F. Bourada, M. Sekkal, S. Zerouati, F. Z. Zaoui, A. Tounsi, A. Derras, A. A. Bousahla, and A. Tounsi. 2019. Analytical study of bending and free vibration responses of functionally graded beams resting on elastic foundation. *Structural Engineering and Mechanics*71(2):185-96.

Chang, W. J., H. L. Lee. 2013. Free vibration of an embedded conical nanotube with surface effect. *Digest Journal of Nanomaterials and Biostructures* 8:1325-1333.

Chen, X., C. Q. Fang, and X. Wang. 2017. The influence of surface effect on vibration behaviors of carbon nanotubes under initial stress. *Physica E* 85:47–55.

Dastjerdi, S. and Y. Tadi Beni. 2019. A novel approach for nonlinear bending response of macro-and nanoplates with irregular variable thickness under nonuniform loading in thermal environment. *Mechanics Based Design of Structures and Machines* 1-26.

Draiche, K., A. A. Bousahla, A. Tounsi, A. S. Alwabli, A. Tounsi, and S. R. Mahmoud. 2019. Static analysis of laminated reinforced composite plates using a simple first-order shear deformation theory. *Computers and Concrete* 24(4):369-78.

Draoui, A., M. Zidour, A. Tounsi, and B. Adim. 2019. Static and Dynamic Behavior of Nanotubes-Reinforced Sandwich Plates Using (FSDT). *Journal of Nano Research* 57:117-135.

Eringen, A. C. 1972. Nonlocal polar elastic continua. *International journal of engineering science* 10:1-16.

Farshi, B., A. Assadi, and A. Alinia-Ziazi. 2010. Frequency analysis of nanotubes with consideration of surface effects. *Applied Physics Letters* 96:093105.

Fattahi, A. M., S. Sahmani, and N. A. Ahmed. 2019. Nonlocal strain gradient beam model for nonlinear secondary resonance analysis of functionally graded porous micro/nano-beams under periodic hard excitations. *Mechanics Based Design of Structures and Machines* 1-30.

Jena, S. K., and S. Chakraverty. 2018a. Free vibration analysis of variable cross-section single layered graphene nano-ribbons (SLGNRs) using differential quadrature method. *Frontiers in Built Environment* 4:63.

Jena, S. K., and S. Chakraverty. 2018b. Free vibration analysis of single walled carbon nanotube with exponentially varying stiffness. *Curved and Layered Structures* 5:201-212.

Jena, S. K., and S. Chakraverty. 2018c. Free vibration analysis of Euler-Bernoulli Nano beam using differential transform method. *International Journal of Computational Materials Science and Engineering* 7:1850020.

Jena, S. K., S. Chakraverty, and F. Tornabene. 2019a. Vibration characteristics of nanobeam with exponentially varying flexural rigidity resting on linearly varying elastic foundation using differential quadrature method. *Materials Research Express* 6:085051.

Jena, S. K., S. Chakraverty, and F. Tornabene. 2019b. Dynamical behavior of nanobeam embedded in constant, linear, parabolic, and sinusoidal types of Winkler elastic foundation using First-Order nonlocal strain gradient model. *Materials Research Express* 6:0850f2.

Jena, S. K., S. Chakraverty, and F. Tornabene. 2019c. Buckling Behavior of Nanobeam Placed in an Electro-Magnetic Field Using Shifted Chebyshev polynomials Based Rayleigh-Ritz Method. *Nanomaterials* 9(9): 1326.

Jena, S. K., S. Chakraverty, R. M. Jena, and F. Tornabene. 2019. A novel fractional nonlocal model and its application in buckling analysis of Euler-Bernoulli nanobeam. *Materials Research Express* 6:055016.

Jena, S. K., S. Chakraverty, and M. Malikan. 2019. Implementation of Haar wavelet, higher order Haar wavelet, and differential quadrature methods on buckling response of strain gradient nonlocal beam embedded in an elastic medium. *Engineering with Computers* https://doi.org/10.1007/s00366-019-00883-1.

Jena, S. K., and S. Chakraverty. 2019a. Differential Quadrature and Differential Transformation Methods in Buckling Analysis of Nanobeams, *Curved and Layered Structures* 6:68-76.

Jena, S. K, and S. Chakraverty. 2019b. Dynamic Behavior of Electro-Magnetic Nanobeam Using Haar Wavelet Method (HWM) and Higher Order Haar Wavelet Method (HOHWM). *The European Physical Journal Plus* 134(10):538.

Jena, S. K., and S. Chakraverty. 2019c. Dynamic Analysis of Single-Layered Graphene Nano-Ribbons (SLGNRs) with Variable Cross-Section Resting on Elastic Foundation. *Curved and Layered Structures* 6(1):132-145.

Jena, S. K., S. Chakraverty, and R. M. Jena. 2019. Propagation of Uncertainty in Free Vibration of Euler-Bernoulli Nanobeam. *Journal of the Brazilian Society of Mechanical Sciences and Engineering* 41(10): 436.

Larbi, L.O., A. Kaci, M. S. A. Houari, and A. Tounsi. 2013. An efficient shear deformation beam theory based on neutral surface position for bending and free vibration of functionally graded beams. *Mechanics Based Design of Structures and Machines* 41(4):421-433.

Lee, H. L., and W. J. Chang. 2010. Surface effects on frequency analysis of nanotubes using nonlocal Timoshenko beam theory. *Journal of Applied Physics* 108:093503.

Li, L., and Y. Hu. 2015. Buckling analysis of size-dependent nonlinear beams based on a nonlocal strain gradient theory. *International Journal of Engineering Science* 97:84-94.

Malikan, M. 2017. Electro-mechanical shear buckling of piezoelectric nanoplate using modified couple stress theory based on simplified first order shear deformation theory. *Applied Mathematical Modelling* 48:196–207.

Malikan, M., and S. Dastjerdi. 2018. Analytical buckling of FG nanobeams on the basis of a new one variable first-order shear deformation beam theory. *International Journal of Engineering & Applied Sciences* 10:21-34.

Malikan, M., F. Tornabene, and R. Dimitri. 2018. Nonlocal three-dimensional theory of elasticity for buckling behavior of functionally graded porous nanoplates using volume integrals. *Materials Research Express* 5:095006.

Malikan, M., V. B. Nguyen, and F. Tornabene. 2018a. Damped forced vibration analysis of single-walled carbon nanotubes resting on viscoelastic foundation in thermal environment using nonlocal strain gradient theory. *Engineering Science and Technology, an International Journal* 21:778-786.

Malikan, M., V. B. Nguyen, and F. Tornabene. 2018b. Electromagnetic forced vibrations of composite nanoplates using nonlocal strain gradient theory. *Materials Research Express* 5: 075031.

Malikan, M., and V. B. Nguyen. 2018. Buckling analysis of piezo-magnetoelectric nanoplates in hygrothermal environment based on a novel one variable plate theory combining with higher-order nonlocal strain gradient theory. *Physica E: Low-dimensional Systems and Nanostructures* 102:8-28.

Malikan, M., R. Dimitri, and F. Tornabene. 2019. Transient response of oscillated carbon nanotubes with an internal and external damping. *Composites Part B: Engineering* 158:198-205.

Malikan, M., V. B. Nguyen, R. Dimitri, and F. Tornabene. 2019. Dynamic modeling of non-cylindrical curved viscoelastic single-walled carbon nanotubes based on the second gradient theory. *Materials Research Express* 6:075041.

Malikan, M. 2019. On the buckling response of axially pressurized nanotubes based on a novel nonlocal beam theory. *Journal of Applied and Computational Mechanics* 5:103-112.

Medani, M., A. Benahmed, M. Zidour, H. Heireche, A. Tounsi, A. A. Bousahla, A. Tounsi, and S. R. Mahmoud. 2019. Static and dynamic behavior of (FG-CNT) reinforced porous sandwich plate using energy principle. *Steel and Composite Structures* 32(5):595-610.

Mehralian, F., Y. Tadi Beni, and M. Karimi Zeverdejani. 2017. Calibration of nonlocal strain gradient shell model for buckling analysis of nanotubes using molecular dynamics simulations. *Physica B: Condensed Matter* 521:102-111.

Murmu, T., and S. C. Pradhan. 2010. Thermal effects on the stability of embedded carbon nanotubes. *Computational Materials Science* 47:721-7.

Pradhan, S. C., and G. K. Reddy. 2011. Buckling analysis of single walled carbon nanotube on Winkler foundation using nonlocal elasticity theory and DTM. *Computational Materials Science* 50:1052–1056.

Semmah, A., H. Heireche, A. A. Bousahla, and A. Tounsi. 2019. Thermal buckling analysis of SWBNNT on Winkler foundation by non-local FSDT. *Advances in Nano Research* 7(2):89.

She, G. L., F. G. Yuan, Y. R. Ren, and W. Sh. Xiao. 2017. On buckling and post buckling behavior of nanotubes. *International Journal of Engineering Science* 121:130-142.

Sun, Dong-Liang, and Xian-Fang Li. 2019. Initial value method for free vibration of axially loaded functionally graded Timoshenko beams with nonuniform cross section. *Mechanics Based Design of Structures and Machines* 47(1):102-120.

Teifouet, M., A. Robinson, and S. Adali. 2017. Buckling of nonuniform carbon nanotubes under concentrated and distributed axial loads. *Mechanical Sciences* 8:299–305.

Thai, H.-T. 2012. A nonlocal beam theory for bending, buckling, and vibration of nanobeams. *International Journal of Engineering Science* 52:56–64.

Wang, B. L., M. Hoffman, and A. B. Yu. 2012. Buckling analysis of embedded nanotubes using gradient continuum theory. *Mechanics of Materials* 45:52–60.

Wang, C. M., Y. Y. Zhang, S. S. Ramesh, and S. Kitipornchai. 2006. Buckling analysis of micro- and nano-rods/tubes based on nonlocal Timoshenko beam theory. *Journal of Physics D: Applied Physics* 39:3904-3909.

Zhen, Y. X. 2017. Wave propagation in fluid-conveying viscoelastic single-walled carbon nanotubes with surface and nonlocal effects. *Physica E: Low-dimensional Systems and Nanostructures* 86:275-279.